



Published in final edited form as:

Mol Pharm. 2015 December 7; 12(12): 4226–4236. doi:10.1021/acs.molpharmaceut.5b00424.

## Nanogel-conjugated reverse transcriptase inhibitors and their combinations as novel antiviral agents with increased efficacy against HIV-1 infection

TH Senanayake<sup>†,‡</sup>, S Gorantla<sup>‡,‡</sup>, E Makarov<sup>‡</sup>, Y Lu<sup>†</sup>, G Warren<sup>†</sup>, and SV Vinogradov<sup>†,\*</sup>

<sup>†</sup>Department of Pharmaceutical Sciences, College of Pharmacy, University of Nebraska Medical Center, Omaha, NE 68198, USA

<sup>‡</sup>Department of Pharmacology and Experimental Neuroscience, College of Medicine, University of Nebraska Medical Center, Omaha, NE 68198, USA

### Abstract

Nucleoside Reverse Transcriptase Inhibitors (NRTIs) are an integral part of the current anti-retroviral therapy (ART), which dramatically reduced the mortality from AIDS and turned the disease from lethal to chronic. The further steps in curing the HIV-1 infection must include more effective targeting of infected cells and virus sanctuaries inside the body and modification of drugs and treatment schedules to reduce common complications of the long-term treatment and increase patient compliancy. Here, we describe novel NRTI prodrugs synthesized from cholesteryl- $\epsilon$ -polylysine (CEPL) nanogels by conjugation with NRTI 5'-succinate derivatives (sNRTI). Biodegradability, small particle size and high NRTI loading (30% by weight) of these conjugates; extended drug release, which would allow a weekly administration schedule; high therapeutic index (>1000) with a lower toxicity compared to NRTIs; and efficient accumulation in macrophages known as carriers for HIV-1 infection are among the most attractive properties of new nanodrugs. Nanogel conjugates of Zidovudine (AZT), Lamivudine (3TC) and Abacavir (ABC) have been investigated individually and in formulations similar to clinical NRTI cocktails. Nanodrug formulations demonstrated 10-fold suppression of reverse transcriptase activity (EC<sub>90</sub>) in HIV-infected macrophages at 2–10, 2–4 and 1–2  $\mu$ M drug levels, respectively for single nanodrugs, dual and triple nanodrug cocktails. Nanogel conjugate of Lamivudine was the most effective single nanodrug (EC<sub>90</sub> 2  $\mu$ M). Nanodrugs showed a more favorable pharmacokinetics compared to free NRTIs. Spared *i.v.* injections of PEGylated CEPL-sAZT alone could efficiently suppress HIV-1 RT activity to background level in humanized mouse (hu-PBL) HIV model.

\*Corresponding author: 986025 Nebraska Medical Center, Omaha NE 68198-6025, USA. ; Email: vinograd@unmc.edu, Tel: 402-559-9362 Fax: (402) 559-9543

#### #Author Contribution

These authors contributed equally to this work.

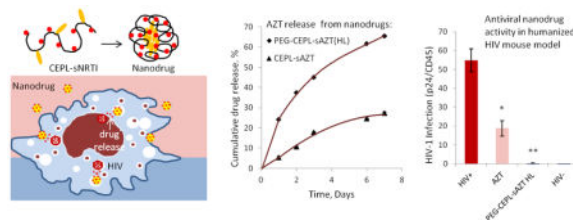
#### Notes

The authors declare no competitive financial interests.

#### Supporting information

Scheme of (PEG)CEPL-sNRTI synthesis (Fig. S1), <sup>1</sup>H-NMR spectra of sAZT (Fig. S2) and s3TC (Fig. S3), as well as data on the *in vitro* AZT release (Fig. S4) and AZT uptake in macrophages (Fig. S5), and also *in vivo* efficacy of CEPL-sNRTI (Fig. S6) are here provided. This material is available free of charge via the Internet at <http://pubs.acs.org>.

## Graphical abstract



## Keywords

HIV-1; nucleoside reverse transcriptase inhibitors; nanogel conjugates; prodrugs of Zidovudine; Lamivudine; Abacavir; epsilon-polylysine; macrophages; mitochondrial toxicity; humanized mouse (hu-PBL)HIV model

## INTRODUCTION

Current anti-retroviral therapy (ART) that uses daily dosage of several antiviral drugs (cocktails) is effective in reducing HIV-1 titer in blood to less than 50 copies/mL and prevents patient mortality; nevertheless, it cannot completely eradicate virus from the body and requires a lifetime application. NRTIs are major components of daily drug cocktails applied to prevent development of virus resistance and enhance antiviral efficiency. From negative point, many patients chronically treated with these drugs often develop a varying degree of myopathy, lipodistrophy, peripheral or central nervous system (CNS) neuropathy. All these side effects are usually associated with mitochondrial toxicity of NRTIs that inhibit DNA polymerase  $\gamma$  and cause mtDNA dysfunction.<sup>1</sup> It can be fatal and is treated by supportive care and discontinuing NRTI. Dose reduction and targeted drug delivery to infected cells represent the most direct way to reduce adverse toxic effects. Recent progress in the development of sub-micron drug delivery systems opens new prospective of introducing more efficient and accommodated to long-term therapy antiviral drugs. Several nanoformulated antiviral drugs, prodrugs and polymer conjugates and different cell-targeting approaches have been evaluated in recent years.<sup>2</sup> Antiviral formulations with a sustained drug release are able to increase patient compliance by offering less frequent administration schedules and by reducing effects of chronic toxicity.<sup>3</sup> In addition, inefficient treatment of HIV-1 infection in the CNS sanctuaries leads to frequent occurrences of neuropathological disorders.<sup>4</sup> HIV-1 infection is located in CD4<sup>+</sup> T cells and productively infected macrophages, however, phagocytosis of dead HIV-infected T cells can lead to the infection of large population of macrophages.<sup>5</sup> In addition, macrophages being present in every organ can disseminate virus to the different sites in the body leading to the formation of viral sanctuaries, including brain-associated macrophages and microglia in the CNS, where integrated HIV-1 was found.<sup>6</sup> Chronic mitochondrial toxicity of NRTIs, particularly in case of Zidovudine and Abacavir, was found to cause neurotoxicity leading to CNS manifestations such as mania and psychosis.<sup>7</sup> Thus, drug formulations with reduced toxicity, which are able to accumulate in infected cells and deliver drugs to HIV-1 sanctuaries, are in high demand.

Recently, we developed novel cationic nanogel carriers for encapsulation of activated NRTIs in the form of 5'-triphosphates and evaluated their anti-HIV activity in macrophages *in vitro* and ability to suppress CNS infection *in vivo*.<sup>8–10</sup> Nanogel-NRTI formulations demonstrated strong affinity to macrophages and reduced mitochondrial toxicity, however, their drug release kinetics required administration three times a week. In order to reduce the frequency of administration, here we propose novel cationic nanogel-NRTI conjugates (prodrugs) and investigate their physicochemical, pharmacological and antiviral properties. For this purpose, we used nanogel particles built from a biodegradable polycationic biopolymer  $\epsilon$ -polylysine (EPL) that have antimicrobial properties and applications in food and cosmetic industry.<sup>11</sup> After EPL modification with hydrophobic moieties of cholesterol and sonication in aqueous media, the modified polycationic polymer (CEPL) formed small nanogel particles. They contain a significant amount of amino groups, which could be conjugated with NRTI molecules. Nanogel-NRTI conjugates (CEPL-sNRTI) can be prepared from 5'-succinyl NRTI (sNRTI) in one simple step. These CEPL-sNRTI prodrugs and their PEGylated counterparts, PEG-CEPL-sNRTI are capable to a sustained NRTI release due to the slower hydrolysis of ester bonds in the conjugates, so that they can be administered less frequently. These nanodrugs demonstrated very low toxicity and strong affinity to macrophages, resulting in targeted and stronger antiviral activity against HIV-1 *in vitro* and *in vivo* compared to free NRTIs. Altogether it makes nanodrugs good candidates for more effective long-term ART.

## MATERIALS AND METHODS

### Materials

All chemical reagents and solvents, if not mentioned separately, were purchased from Sigma-Aldrich (St. Louis, MO) with the highest available purity and used without purification unless otherwise indicated. Epsilon-polylysine was purchased from Tecoland Corporation (Edison, NJ). The mPEG-NHS ester was purchased from JenKem Technology USA (Allen, TX). Cholesterol was purchased from Sigma-Aldrich (St. Louis, MO), N-Succinimidyl [2,3-<sup>3</sup>H] propionate was obtained from Moravak Radiochemical (Brea, CA). Zidovudine (AZT), Lamivudine (3TC), Abacavir (ABC) and N-(3-dimethylaminopropyl)-N'-ethyl carbodiimide hydrochloride (EDC) were purchased from Carbosynth (Newbury, UK). NAP-10 and NAP-25 columns for gel filtration were purchased from GE Healthcare Biosciences (Piscataway, NJ). Dialysis tubes were obtained from Thermo Fisher Scientific (Waltham, MA). <sup>1</sup>H-NMR spectra were recorded in d-DMSO at 25°C using a 500 MHz Varian NMR spectrometer. All chemical shift values are given in parts per million (ppm) and are referenced to a signal from tetramethylsilane. Hydrodynamic diameter, polydispersity, and zeta-potential were measured by a dynamic light scattering (DLS) using Zetasizer Nano-ZS90 (Malvern Instruments) with a 15 mV solid state laser operated at a wavelength of 635 nm. UV-absorbance was measured by Biophotometer (Eppendorf) or NanoDrop 2000 spectrophotometer (Thermo Fisher Scientific). Transmission electron microscopy (TEM) was performed after contrast vanadate staining of samples using a FEI Tecnai G2 Spirit electron microscope (Hillsboro, OR).

## Cells

Human HepG2 hepatocellular carcinoma cells were purchased from American Type Culture Collection (Manassas, VA) and cultivated in Eagle's Minimal Essential Medium (MEM, Corning Cellgro) containing 10% heat-inactivated fetal bovine serum (FBS) supplemented with streptomycin (5  $\mu\text{g}/\text{mL}$ ). Primary human monocytes and peripheral blood leukocytes (PBL) were obtained from leukopheresis of HIV-seronegative donors, then purified by the countercurrent centrifugal elutriation as previously described.<sup>12</sup> Monocytes were differentiated into MDM by culturing in DMEM supplemented with 10% heat-inactivated pooled human serum and 1% glutamine, 10 mg/mL ciprofloxacin and 1,000 U/mL of purified recombinant human macrophage colony-stimulating factor (R&D Systems). A macrophage-tropic CCR5-utilizing viral strain HIV-1<sub>ADA</sub> at a multiplicity of infection (MOI) of 0.01 was amplified and used for the infection of cells at a TCID<sub>50</sub> (tissue culture 50% infective dose) of 10<sup>4</sup>.

## Synthesis of nanodrugs

**Synthesis of CEPL nanogels**—EPL (4.7 g, 1 mmol) was mixed with in 15 mL of anhydrous DMSO and sonicated for 15–30 minutes to completely dissolve. Cholesterol chloroformate (19.1 mg, 0.05 mmol) in dichloromethane (1 mL) was added drop wise over 30 min under argon. The final mixture was stirred overnight at 25°C, filtered, and concentrated *in vacuo*. The CEPL product was dialyzed in semi-permeable tubes (MWCO 3.5 kDa) against 20% ethanol two times for 24 h at RT, then concentrated *in vacuo* and isolated with an 80% yield. The solution was adjusted to pH 7 by 1M hydrochloric acid. <sup>1</sup>H-NMR spectrum (d<sub>6</sub>-DMSO);  $\delta$ : 0.34(s, 9H), 0.53(m, 18H), 0.58(m, 9H), 0.66(m, 9H), 0.83–1.0 (m, 60H), 1.09–1.12 (m, 60H), 1.19–1.31 (m, 60H), 2.75–2.76 (m, 60H), 3.07 (s, 30H). PEG-modified nanogel (PEG-CEPL) was prepared as follows: CEPL (0.575 mg 0.095  $\mu\text{mol}$ ) was dissolved in 1.5 mL water (solution pH, 7.5), then solution of mPEG<sub>5000</sub>-NHS linker (1.9 g, 0.38 mmol) was added and the mixture was incubated for 2h at 25°C. PEGylated CEPL nanogel was isolated by dialysis (MWCO 8–12 kDa), lyophilized and isolated with a yield 78%. <sup>1</sup>H-NMR spectrum (d<sub>6</sub>-DMSO);  $\delta$ : 0.35 (s, 9H), 0.53 (m, 18H), 0.58 (m, 9H), 0.66 (m, 9H), 1.0 (m, 60H), 1.11 (m, 60H), 1.21–1.32 (m, 60H), 2.76 (m, 60H), 2.93 (s, 30H), 3.20–3.23 (m, 1816H).

**Synthesis of NRTI 5'-succinates**—A mixture of AZT (2.67 g, 10 mmol), succinic anhydride (1.50 g, 15 mmol) and 4-dimethylaminopyridine (DMAP) (1.221 g, 10 mmol) in dry dichloromethane (100 mL) was stirred at room temperature for 18 h. The solvent was evaporated *in vacuo*, and product was purified by flash chromatography on silica gel column using a concentration gradient of methanol (0 to 20% v/v) in dichloromethane as an eluent. The same procedure was used in the synthesis of sABC and s3TC. Fractions containing 5'-succinylated NRTI were collected, concentrated *in vacuo* and isolated with a yield of 67–70%. <sup>1</sup>H-NMR spectra (d<sub>6</sub>-DMSO): **sAZT**,  $\delta$ : 1.61 (s, 3H), 2.16–2.40 (m, 6H), 3.79 (m, 1H), 4.09 (m, 2H), 4.26 (m, 1H), 5.94(t,  $J=6.5$  Hz, 1H), 7.21 (s, 1H), 11.16 (s, 1H), 12.07 (s, 1H). **sABC**,  $\delta$ : 0.38–0.45 (m, 4H), 1.42 (m, 1H), 1.64 (m, 2H), 2.45 (m, 1H), 2.84 (m, 2H), 3.80 (m, 1H), 3.60 (m, 2H), 3.92 (s, 2H), 5.20 (s, 1H), 5.64–5.74 (d, 2H), 5.88 (s, 1H), 7.21 (s, 2H), 7.43 (s, 1H), 12.00 (brs, 1H). **s3TC**,  $\delta$ : 1.04 (s, 6H), 2.45 (m, 1H), 2.58 (m, 2H), 2.65

(m, 1H), 3.24 (m, 2H), 3.60 (m, 2H), 4.45 (m, 2H), 5.40 (s, 1H), 6.20 (s, 1H), 7.24 (d,  $J=7.5$  Hz, 2H), 8.20 (d,  $J=7.2$  Hz, 2H), 10.85 (s, 1H), 12.2 (s, 1H).

**Synthesis of CEPL-sNRTI conjugates**—The sAZT (68 mg, 0.18 mmol) was mixed with CEPL (74 mg, 0.012 mmol, 0.362 mmol of amino groups) in 50% aqueous DMF (4 mL), and pH was adjusted to 6.5–7.0. Then, EDC (70 mg, 0.366 mmol) was added to this mixture, and the reaction was continued overnight at RT. CEPL-sAZT conjugate was isolated by dialysis (MWCO 3.5 kDa) against water overnight at 4°C. The aqueous solution was sonicated for 30 min and lyophilized. The isolated yield of nanogels in lyophilized form was near 75%. The CEPL-sABC and CEPL-s3TC were synthesized according to the procedure used to synthesize CEPL-sAZT. Drug content was calculated based on their UV spectra (extinction coefficients: AZT,  $\epsilon_{260}=9700$ ; ABC,  $\epsilon_{280}=12264$  and 3TC<sup>ibu</sup>,  $\epsilon_{260}=9476$ ) and correlated by the absorbance of non-modified CEPL carrier. Nanodrugs with the drug content of 0.7–0.93  $\mu\text{mol}/\text{mg}$  were obtained (Table 1).

### In vitro drug release

*In vitro* drug release studies were performed as follows.<sup>13</sup> Solutions of nanodrugs (10 mg/1 mL) were placed in small dialysis tubes (MWCO 3.5 kDa) and immersed in 150 mL of PBS (pH 7.4) containing 0.1% sodium azide. During incubation at 25°C under slow stirring, 5  $\mu\text{L}$  aliquots were withdrawn from the sample solution at selected time points and replaced with equal volume of PBS, and their UV absorbance was measured at 260 nm in triplicate using NanoDrop (Thermo Scientific). Free NRTI drug release from the dialysis tube was fast enough and complete in 6 h at these conditions (Figure S4). Data were expressed in the form of cumulative drug release vs. incubation time.

### Cellular accumulation

Cellular accumulation was studied in human monocyte-derived macrophages (MDM). CEPL nanogel was tagged with Rhodamine (Rh) isothiocyanate and purified as previously described.<sup>14</sup> MDM suspension ( $1 \times 10^6$  cells/mL) was treated with nanodrug concentrations of 10 and 50  $\mu\text{g}/\text{mL}$  in full cell medium. At appropriate time intervals, samples were taken ( $10^5$  cells) and washed with cold PBS, then treated with propidium iodide for 15 minutes at 4°C and analyzed by fluorescence-activated cell sorting (FACS). The percentage of live cells and the mean fluorescent intensity was measured using FACS Array Bioanalyzer (BD Bioscience). As a control, AZT accumulation was measured in treated cells (in triplicates) after two freeze-thaw cycles and ultrasonic cell disintegration. UV absorbance in supernatant after spinning cell debris was measured at 260 nm using NanoDrop (Thermo Scientific). All data were corrected for absorbance of untreated cells and normalized by protein content measured using Pierce's BCA Protein Assay. Results were expressed in the form of cumulative drug accumulation vs. incubation time (Figure S5).

Intracellular drug release from nanodrugs was determined in MDM cells. MDM ( $5 \times 10^6$  cells per well) were cultured in 15 cm dish at 37°C for 24–48 h until cell confluency of 80%. Cells were treated with PEG-CEPL-sAZT (0.5 mg/mL, 4 h at 37°C) and then incubated in fresh medium for different time periods (8, 24 and 48 h); sampled cells were washed 3 times with phosphate buffered saline (PBS) and stored at –80°C. Thawed cells were treated with

methanol and centrifuged to remove debris and dried *in vacuo*. Samples were then analyzed in triplicates by reverse phase HPLC on Ascentis C18 column (10  $\mu\text{m}$ , 15 cm $\times$ 4.6 mm) (Sigma-Aldrich) using UV detection at 260 nm and flow rate of 1 mL/min. The HPLC was performed in standard conditions of the peptide analysis using buffers A (20 mM TFA in water) and buffer B (30% acetonitrile, 20 mM TFA in water) in a linear gradient mode (0 to 100% B in 20 min). Nanodrug concentration after integration was determined by comparison to a standard curve for nanodrug dilutions.

### Cytotoxicity

Cytotoxicity of NRTIs and corresponding nanodrugs was evaluated using a MTT assay as previously described.<sup>14</sup> Initially, MDMs were treated for 4 h at 37°C to allow the internalization of nanodrugs, then the treatment solution was washed out, and cells were incubated for additional 48 h at 37°C. MTT assay was also used in the measurements of viral RT activity in HIV-1 infected MDMs in order to normalize virus inhibition data by the drug cytotoxicity.

### Mitochondrial toxicity

Effect of the extended treatment of hepatic HepG2 cells with AZT and corresponding nanodrugs on the level of mtDNA was measured as previously described.<sup>10</sup> Cells were treated with sterile solutions of AZT (30  $\mu\text{g/mL}$ ) or CEPL-sAZT nanodrug (30% AZT content, 100  $\mu\text{g/mL}$ ) in full medium for 4 h at 37°C on Days 1, 4 and 7, and analyzed on Day 10. After trypsinolysis and treatment with RNase, DNA samples were isolated and analyzed by a SYBR Green real-time PCR. Cytochrome *b* gene (mtDNA): 5'-CCAACATCTCCGCATGATGAAAC-3' (direct) and 5'-GTGGGCGATTGATGAAAAGG-3' (reverse), and  $\beta$ -actin gene (nuDNA): 5'-AACACCCCAGCCATGTACGT-3' (direct) and 5'-TCTCCTTAATGTCACGCACGA-3' (reverse) primers were applied to quantify the amount of mtDNA and nuDNA.<sup>15</sup> Mini-iQ Real-Time PCR detection system and Evagreen Supermix at the conditions recommended by the manufacturer (BioRad) have been used in the analysis. The results were calculated as a relative expression of mtDNA compared to nuDNA ( $E_{\text{rel}}$ ) using an equation:

$E_{\text{rel}} = 2^{-C(t)_{\text{mt}}} / 2^{-C(t)_{\text{nu}}}$ , where  $C(t)_{\text{mt}}$  and  $C(t)_{\text{nu}}$  are the quantification cycles observed for mtDNA and nuDNA in the same amount of sample DNA.

### Reverse transcriptase inhibition

Human MDM were cultured for 7 days in 96-well plates, changing culture medium every other day. Individual nanodrugs, dual nanodrug (CEPL-sAZT, CEPL-s3TC, 2:1) and triple nanodrug (CEPL-sAZT, CEPL-s3TC, CEPL-sABC, 2:1:2) formulations and NRTI alone were dissolved in sterile deionized water to obtain 20x stock solutions. In sterile 96-well plate, 10  $\mu\text{L}$  of the stock solutions were mixed with 190  $\mu\text{L}$  of complete culture medium, and serial 1/2 dilutions (100  $\mu\text{L}$ ) were prepared. On Day 7, old media was removed and supplemented with the serial dilutions. Plates were incubated for 4 h at 37°C and 5%  $\text{CO}_2$ . After incubation, cells were washed with PBS, and the fresh media containing 0.01 MOI of HIV-1<sub>ADA</sub> was added for the overnight (16 h) infection. Infected MDMs were washed and supplemented with a fresh medium. On Days 7 and 10 post-infection, supernatants were



collected for the RT activity assay. Each plate contained infected but non-treated and uninfected cell controls. All drugs concentrations and controls were analyzed in five parallels.

To measure HIV-1 replication, reverse transcriptase (RT) activity was determined by incubating 10  $\mu\text{L}$  of infected sample media with a reaction mixture consisting of 0.05% Nonidet P-40 (Sigma-Aldrich) and [ $^3\text{H}$ ]-dTTP (2 Ci/mmol; Moravek) in tris-HCl buffer (pH 7.9) for 24 h at 37°C on days 7 and 10 post-infection.<sup>12</sup> Radiolabeled DNA was precipitated on paper filters in an automatic cell harvester (Skatron) and incorporated activity was measured by liquid scintillation spectroscopy. The cytotoxicity of nanodrugs was determined using an MTT assay as previously described. The mean OD<sub>490</sub> values for non-treated controls were taken for 1, and the cytotoxicity data have been converted to obtain the normalization factors. All observed HIV-1 RT activity values were normalized by the cytotoxicity data and plotted as a function of nanodrug or NRTI concentrations and ratios in multidrug combinations. Antiviral efficacy was determined from these curves using GraphPad Prism 4.03 (GraphPad Software) and expressed as an effective drug concentration that inhibited HIV-1 RT activity by a factor of 10 (EC<sub>90</sub>).

## Hemolysis

Human whole blood samples (1 mL) were transferred into heparinized tubes and precipitated by centrifugation at 2000 rpm for 10 min. Supernatant was discarded and pellets were washed three times with PBS and re-suspended to a concentration of  $7.5 \times 10^6$  cells/mL. The 50  $\mu\text{L}$  of red blood cell (RBC) suspensions were added to 100  $\mu\text{L}$  solutions of nanogel or nanodrugs in PBS at the concentrations ranging from 0.0014 to 1 mg/mL. These samples were incubated at 37°C for 1 h and centrifuged at 2000 rpm for 5 min. Released hemoglobin was determined by the spectrophotometry at 415 nm. As a negative control (complete hemolysis), the RBC suspension was treated with distilled water. The degree of hemolysis was calculated according to the following equation:

Hemolysis (%) =  $(A - B) \times 100 / (C - B)$ , where A, B, C are absorbance of the sample, positive (PBS), and negative (water) controls, respectively.

## Pharmacokinetics

CEPL-sAZT nanodrug was tagged with N-succinimidyl [2,3- $^3\text{H}$ ] propionate (less than 2% amino groups in EPL) via formation of stable amide bonds and then purified using gel-filtration through NAP-10 column as previously described.<sup>14</sup>  $^3\text{H}$ -labeled CEPL-sAZT nanodrug (250  $\mu\text{g}$ , 30% AZT content) or  $^3\text{H}$ -AZT (75  $\mu\text{g}$ , Moravek Radiochemical) were *i. v.* injected to Balb/c mice. Routinely, animals were randomly divided into groups of no more than five mice per cage and maintained under sterile conditions in controlled environment. All manipulations with animals were performed in a sterile laminar hood using sterile solutions. Animal studies were performed according to the principles of animal care outlined by the National Institutes of Health, and protocols were approved by the Institutional Animal Care and Use Committee at the University of Nebraska Medical Center. At predetermined time points (0.5, 1, 2, 8, and 24 h groups, n = 3) mice were sacrificed, and blood and urine were collected. The blood was centrifuged to obtain plasma (2500 g, 5 min at 4°C). Plasma and urine were treated with 10% methanol for 10 min and then centrifuged (2500 g, 5 min)

to remove proteins. The supernatant was dried and dissolved in Ultima Gold (Sigma) scintillator cocktail, and tritium radioactivity was analyzed using a Packard liquid scintillation counter. Plasma kinetic parameters of CEPL-sAZT and AZT were calculated from the drug concentration–time curves. The maximum plasma concentration ( $C_{\max}$ ) and the time to reach  $C_{\max}$  ( $t_{\max}$ ) were obtained directly from the drug concentration–time data. The area under the concentration–time curve (AUC) was used as a measure of total amount of CEPL-sAZT that reached systemic circulation. AUC from time zero to the last sampling time ( $AUC_{0-t}$ ) was calculated by the trapezoid rule. The elimination rate constant,  $k_{el}$ , was obtained from the slope of the drug concentration–time curve. The elimination half-life ( $t_{1/2}$ ) was calculated as 0.693 divided by  $k_{el}$ . Drug clearance (CL) is the volume of plasma in the vascular compartment cleared of drug per unit time.

### Antiviral activity in vivo

In preliminary testing the antiviral activity of new nanodrugs *in vivo*, an established humanized PBL-NSG mouse model of HIV-1 infection was used.<sup>16</sup> NOD/scid- $\gamma_c^{\text{null}}$  (NSG) mice aged 4–5 weeks were purchased from Charles River Laboratories (Wilmington, MA), then reconstituted with human peripheral blood lymphocytes (hu-PBL) after injection of  $2 \times 10^7$  cells in total volume not exceeding of 300  $\mu\text{L}$  PBS solution into the mouse peritoneal cavity. Seven days after, PEG-CEPL-sAZT (100 mg/kg) or equivalent amount of AZT were *i.v.* injected 4 h prior *i.p.* HIV-1<sub>ADA</sub> infection with a 50% tissue culture infectious dose (TCID<sub>50</sub>) of  $10^4$ . AZT and nanodrug were given three times over 15 days period. HIV-1 infected but PBS injected animals served as controls. Anti-retroviral activity was evaluated by the determination of virus suppression and preservation of CD4<sup>+</sup> T cells. HIV-1 *gag* RNA by real-time polymerase chain reaction (RT-PCR) in spleen and immunohistochemical quantitation of infected cells by staining for HIV-1p24 proteins was assessed using a PBL marker CD45. Two independent experiments were carried out in order to determine statistically significant suppression of viral replication compared to non-treated control and AZT alone.

## RESULTS

### Synthesis and characterization of nanogel-drug conjugates

The general structure of (PEG) CEPL-sNRTI nanodrugs is shown in Figure 1. 5'-Succinyl NRTIs have been obtained by the reaction of nucleoside analog with succinic anhydride and used as intermediates in the synthesis of nanodrugs. Before the synthesis, an exocyclic amino group of Lamivudine was protected by acylation with isobutyryl anhydride to increase the yield and purity of the corresponding succinylated N-isobutyl Lamivudine (s3TC).<sup>13</sup> CEPL-sNRTI conjugates could be readily obtained from CEPL and sNRTI in aqueous medium in the presence of water-soluble carbodiimide (EDC) with high NRTI loading (28–30%). Nanodrugs are easily purified by dialysis and can be lyophilized. To extend *in vivo* circulation time and reduce renal clearance, the CEPL nanogel could be PEGylated with an mPEG-NHS reagent in a 1:4 molar ratio. Reaction between this reagent and amine groups of CEPL proceeded with a yield > 90% and resulted in the formation of stable *in vivo* amide bonds. All nanodrugs demonstrated good dispersibility in water (Table 1).



Quantitative analysis of products was performed by  $^1\text{H}$ -NMR and UV spectroscopy. The integrated signals for cholesterol methyl group (0.34 ppm),  $\alpha$ -protons of EPL (3.07 ppm), and methylene protons of PEG (3.23 ppm) have been selected for the calculation of cholesterol and PEG content. According to our data, cholesterol content in the CEPL nanogel was 28% and the PEG : CEPL molar ratio in the PEG-CEPL conjugate was equal to 3.6 : 1, which was close to the stoichiometry (4 : 1) used in the modification. Nanodrugs with lower (LL) and higher NRTI loading (HL) have been synthesized and studied; the NRTI loading in nanodrugs was calculated based on their UV absorbance using extinction coefficients of the corresponding NRTIs. We could load in the nanogel network a significant amount of antiviral drugs (up to 28–30% wt). CEPL-sNRTI and PEG-CEPL-sNRTI formed small uniform particles after ultrasonication in aqueous media. Particle size, polydispersity and zeta-potential of nanogels and nanodrugs were measured by the dynamic light scattering (DLS) (Table 1). Nanodrugs showed a spherical morphology as determined by transmission electron microscopy (TEM, Figure 2A). Lyophilized samples reconstituted in water demonstrated similar properties after the storage.

### ***In vitro* drug release**

Drug release from CEPL-sAZT, PEG-CEPL-sAZT (LL) and (HL) nanodrugs occurring due to the cleavage of succinate linker was monitored in PBS (pH 7.4) at 37°C in ‘open sink’ conditions. All nanodrugs showed a drug release kinetics that directly depended on drug content (Figure 2B). The fastest AZT release was observed from PEG-CEPL-sAZT (HL) ( $t_{1/2}$  4 days), and the slowest AZT release was from CEPL-sAZT. Evidently, the positively charged amino groups in CEPL affect the process. Amino group modifications with drug and PEG molecules diminish the charge, also resulting in the reduction of particle size as shown in Table 1. Thus, at physiological pH, drug release is fairly slow and extends over 7 days. It would allow to use the new nanodrugs in less frequent drug administration protocols. Linker degradation and drug release progress from the exterior of spherical particles toward its interior, therefore, drug release kinetics was faster in the beginning and slower later in time (Figure 2B). This explains well the observed shapes of these curves.

### **Uptake and drug release in macrophages**

Although, the major HIV-infected cellular targets to antiviral therapy are CD4+ T cells, macrophage population represents a significant latent reservoir of HIV-1 infection in the CNS and, due to the phagocytosis of infected T cells, also in the body.<sup>5</sup> Our major focus is on the therapeutic treatment of HIV-1 infection in the CNS, therefore, we primarily evaluated nanodrug accumulation in an *in vitro* culture of human monocyte-derived macrophages (MDM). Cultured MDM were treated with Rhodamine-labeled CEPL nanogels and analyzed at several time points by fluorescence-activated cell sorting (FACS). We observed a substantial nanogel accumulation in MDM compared to its concentration in the medium (50  $\mu\text{g}/\text{mL}$ ). For comparison, the kinetics of AZT accumulation in MDM is shown in Figure S5. As per drug, nanodrug could deliver a more than twice higher amount of AZT inside the cells compared to free AZT accumulation after 4h-treatment. At lower nanodrug concentration (10  $\mu\text{g}/\text{mL}$ ), the observed accumulation was even more selective (17-fold increase). MDM showed an initial fast uptake of nanodrugs that mostly reached

saturation after 4h-treatment (Figure 3A, B). This time was used for MDM pretreatment before HIV-1 infection in the consequent nanodrug antiviral activity experiments.

Nanodrug degradation within MDM was assessed at several time points by reverse phase HPLC after 4h-pretreatment of cells with PEG-CEPL-sAZT (HL). Figure 3C shows a gradual drop in the nanodrug concentration, which however remained at active antiviral levels ( $> 5 \mu\text{g/mL}$ ) for at least 9 days. We observed a comparable 40% drug release from nanodrugs *in vitro* and in macrophages after the first two days (Figure 2B and 3C).

### Cytotoxicity

Cytotoxicity of nanodrugs was measured in MDM using a standard MTT cell viability assay. MDM have been pretreated for 4 h with serial dilutions of NRTIs or nanodrugs in order to allow accumulation of nanodrugs in macrophages and analyzed 48 h later. Plotted cell viability curves were used to calculate nanodrug concentrations when 50% of treated cells survive ( $\text{IC}_{50}$  values) (Figure 4A–C). Nanodrugs demonstrated very good cytotoxicity profile that was better or comparable to free NRTIs.  $\text{IC}_{50}$  values for NRTI, CEPL-sNRTI and PEG-CEPL-sNRTI were equal to 0.5, 1 and 2 mg/mL, respectively, in AZT series and 2.5, 3 and  $>3$  mg/mL in 3TC series. Thus, nanodrugs exhibited lower cytotoxicity than corresponding free NRTIs.

Mitochondrial toxicity of nanodrugs was evaluated after a long-term treatment of HepG2 cells, an established model for drug comparison. Cells were treated over the period of 10 days and total DNA was isolated. Normally, the ratio of mitochondrial DNA (mtDNA) and nuclear DNA (nuDNA) is high and constant for each specific cell type. Inhibition of mtDNA synthesis results in the reduction of this ratio. When AZT and the corresponding CEPL-sAZT and PEG-CEPL-sAZT nanodrugs were compared at equal AZT concentrations, we observed a 60% drop of the mtDNA amount in AZT-treated samples, but only a 35% drop in nanodrug-treated samples. Thus, mitochondrial toxicity of nanodrugs was nearly two times lower compared to AZT (Figure 4D). Overall, our data show that nanodrugs have much lower cytotoxicity and mitochondrial toxicity than free NRTI counterparts.

### Antiviral activity

Antiviral efficiency of nanodrugs and multi-drug cocktails was compared by their effect on a dose-dependent reverse transcriptase (RT) activity measured in HIV-1 infected MDMs at different time points post-infection. The cells were pretreated with nanodrugs for 4h before inoculation with HIV-1<sub>ADA</sub> strain. Viral RT activity in treated and non-treated HIV-1 infected MDMs was analyzed by inclusion of  $^3\text{H}$ -thymidine in DNA on Days 7 and 10. Antiviral efficacy of CEPL-sAZT, CEPL-s3TC and CEPL-sABC, and their mixtures corresponding to clinical Trizivir (AZT: 3TC: ABC, wt ratio 2:1:2) and Combivir (AZT: 3TC, wt ratio 2:1) cocktails. Individual nanodrugs of AZT or ABC induced 10-fold suppression of HIV-1 RT activity ( $\text{EC}_{90}$ ) at concentrations  $7 \mu\text{g/mL}$  ( $23\text{--}27 \mu\text{M}$ ), while CEPL-s3TC was the most effective single nanodrug having an  $\text{EC}_{90}$   $0.12 \mu\text{g/mL}$  (Figure 5A–D). Nanodrugs show an equivalent or better antiviral activity compared to free drugs based on the NRTI content in nanodrugs (20–30%). Thus, nanodrugs demonstrated an equal antiviral effect at NRTI concentrations 3–5 times lower than free NRTIs. Dual nanodrug

cocktail showed virus inhibition at two times lower EC<sub>90</sub> of 3TC (0.06 µg/mL) than nanodrug of 3TC alone (0.12 µg/mL). Triple nanodrug cocktail was the most effective, demonstrating an effective virus inhibition at three times lower EC<sub>90</sub> of 3TC (0.04 µg/mL) (Figure 5D). Nanodrug combinations demonstrated an excellent activity and suppressed HIV-1 RT activity to the minimal detection sensitivity of the assay. When antiviral activity of AZT was compared to Trizivir-like cocktail and PEG-CEPL-sAZT was compared to the corresponding triple nanodrug cocktail at a fixed concentration of 4 µg/mL, the 10-fold virus inhibition in the infected MDM was achieved only after the treatment with nanodrugs (Figure 5E).

## Hemolysis

The hemolytic properties of nanodrugs were investigated by spectrophotometric evaluation of the hemoglobin released from human erythrocytes (RBC) after the treatment with increasing levels of CEPL-sAZT and PEG-CEPL-sAZT (Figure 6A). For comparison, the test was carried out with the initial non-substituted CEPL nanogel. According to our data, CEPL possessed a strong dose-dependent hemolytic activity due to the cationic nature of the carrier. However, following the conjugation with sNRTI, the cationic charge of nanodrug can be significantly reduced (Table 1). Compared to CEPL, (PEG)CEPL-sNRTI conjugates displayed a 7-fold lower level of hemolysis at the concentration of 1 mg/mL and no adverse effect at the lower levels (0.2 mg/mL) in the blood.

## Pharmacokinetic properties

*In vivo* properties of <sup>3</sup>H-labeled CEPL-sAZT have been evaluated in mice after tail vein injection. We observed a significantly improved pharmacokinetics of the nanodrug compared to free AZT in the blood (Figure 6B). Pharmacokinetic parameters calculated from these curves are shown in Table 2. Area under the curve (AUC) was 2.5 times larger, half-life time (t<sub>1/2</sub>) was 3 times longer and clearance rate (CL) was 2 times slower for the injected nanodrug compared to AZT. During this experiment, we observed that <70% of nanodrug was excreted with urine 24 h after *i.v.* injection (data not shown). For comparison, more than 90% of administered AZT is removed with urine.<sup>17</sup> Though, the clearance of the nanodrug was slower, it was not surprising since the calculated M.w. of CEPL-sAZT (ca. 9 kDa) was lower than the kidney excretion limit (ca. 40 kDa). Pharmacokinetic properties of nanodrugs could be improved by PEGylation that is known to increase the circulation time of nanocarriers in blood and reduce interaction with plasma proteins. Administration of vectorized PEGylated nanodrugs is also necessary for the efficient nanodrug delivery into the brain. Thus, PEGylated CEPL-sNRTI nanodrugs have been chosen for the next *in vivo* experiments in order to evaluate how effective was the *i.v.* injection of new nanodrugs in the treatment of HIV-1 infection.

## Antiviral activity *in vivo*

Antiviral activity of novel nanodrugs was evaluated in humanized mouse model of HIV-1 infection: HIV-1<sub>ADA</sub>-infected NOD/scid-γ<sub>c</sub><sup>null</sup> (NSG) mice reconstituted with human peripheral blood lymphocytes (PBL) (PBL-NSG mice)<sup>16</sup>. NSG mice (groups of 5) were reconstituted by injecting 20 million human PBL intraperitoneally (*i.p.*). Seven days after human cell reconstitution, either AZT nanodrug or free AZT (at equal AZT dosage) were *i.v.*

injected 4 hours before HIV-1<sub>ADA</sub> infection. The virus was injected *i.p.* at 10<sup>4</sup> 50% tissue culture infectious dose (TCID<sub>50</sub>). Mice received two more *i.v.* injections of AZT nanodrug or AZT on Days 5 and 10 post-infection. Animals were perfused in the end of experiment on Day 15; their brains were sampled and sectioned for immunostaining by HIV-1 anti-p24 and lymphocyte anti-CD45 antibodies. Treatment of mice with a triple nanodrug (CEPL-sNRTI) cocktail demonstrated better inhibition of HIV-1 than a triple drug cocktail and resulted in 2.5-fold reduction of the virus level per lymphocyte (p24/CD45); however, this result was not statistically significant (Figure S6). In contrast, application of PEG-CEPL-sAZT(HL) with a slightly lower drug content (25%) was successful. Figure 6C shows the virus level per lymphocyte (p24/CD45) before and after the treatment. We observed a three-fold reduction in the HIV-1 level after the applied therapy using AZT ( $P < 0.05$ ), while the nanodrug demonstrated very efficient and statistically significant antiviral activity ( $P < 0.01$ ) reducing HIV-1 infection to barely detectable levels. As the next step of these studies, we plan to optimize CNS delivery of nanodrugs using vectorization with brain-binding peptides and application of the most effective nanodrug cocktails. Based on our data, we expect that administration of vectorized PEG-CEPL-NRTI prodrugs once a week will be able to suppress not only HIV-1 infection in T cells due to the NRTI release in the blood, but also more efficiently control HIV-1 infection in the CNS where the virus is harbored in the brain macrophages and microglia.

## DISCUSSION

Efficacy of ART depends on the specific accumulation of antiviral drugs in major types of HIV-infected cells, human macrophages and lymphocytes. Small drug molecules like NRTIs that have been selected due to their high therapeutic index do not accumulate preferentially in both types of cells, although they are able to provide effective suppression of the virus to background levels in blood after a daily dose without significant toxicity to infected cells and other organs. However, this treatment cannot eradicate virus completely from the body and patients are obliged to maintain the ART regimen all over their life. This clinical reality results in frequent noncompliance, appearance of resistant HIV-1 strains and chronic toxicity leading to patient impairments. New drug development should be focused on effective targeting of infected cells, drug modifications and long-term acting formulations in order to reduce drug toxicity and administration frequency. Here, we report our attempt to enhance the current ART using nanogel-NRTI conjugates as newly designed drug delivery systems. Our approach is based on the application of cationic nanogel carriers, which demonstrated recently an efficient delivery of preactivated NRTI, e.g. AZT 5'-triphosphate (AZT-TP), into HIV-infected macrophages (MDM).<sup>9,10</sup> MDM preferentially capture these cationic nanodrugs, which results in the accumulation of antiviral drugs in the sites of virus multiplication. Recently, we introduced biodegradable compact nanogel particles of amphiphilic cholesteryl- $\epsilon$ -polylysine (CEPL) prepared from non-toxic medium-sized  $\epsilon$ -polylysine (4.6 kDa).<sup>8</sup> Similar approach to encapsulation of AZT-TP in cationic chitosan nanoparticles (NPs) was proposed by means of ionotropic gelation leading to high drug loading efficacy.<sup>18</sup> Incorporation of 3TC and AZT in PLGA-Poloxamer 188 NPs and glycerol monostearate-Poloxamer 188 lipid NPs was able to re-route drug distribution to RES organs rich in macrophages, such as liver and spleen. Lipid NPs also showed a higher

accumulation in these organs than simple NPs.<sup>19</sup> Our CEPL nanogels contain ca. 25% by weight of hydrophobic cholesterol moieties and equally demonstrate high levels of accumulation in macrophages.

Expression of multidrug transporters can significantly limit accumulation and anti-HIV activity of NRTI and other antiviral drugs in infected human macrophages and lymphocytes.<sup>20</sup> Levels of MDR1, MRP4 and MRP5 drug efflux transporters became high following NRTI treatment. Efflux of AZT involved mostly MRP4 and MRP5 transporters and could be effectively reduced by the targeted inhibition of MRP4 expression.<sup>21</sup> Bypassing of multidrug resistance can be achieved by application of prodrugs, which are not recognized by these transporters and therefore can offer more effective treatment against HIV-1 infection.

Many macromolecular prodrugs of NRTI have been studied during the last 15 years.<sup>22</sup> Polysaccharide prodrugs of AZT were found as good candidates for targeting of infected blood cells. AZT conjugates covalently bound through a succinate diester spacer with kappa-carrageenan, a well-tolerated biopolymer used in the food industry, demonstrated an improved anti-HIV activity compared to free AZT *in vitro*.<sup>23</sup> The succinate linker was also successfully used in the preparation of 3TC-dextran (25 kDa) conjugate with improved *in vivo* properties and distribution.<sup>24</sup> This dextran-drug conjugate had a 40 times slower clearance that resulted in higher accumulation and a sustained drug release in liver. In similar AZT-dextrin conjugate, 78.4% of AZT was released in human plasma after 24 h and completely after 48 h.<sup>25</sup> Pharmacokinetic study of this conjugate after *i.v.* administration showed an extension of the plasma half-life and the mean residence time for AZT. Thus, many macromolecular NRTI conjugates (prodrugs) demonstrated high potential as anti-HIV drugs with better pharmacokinetic and extended drug release properties.

In our studies, we prepared 5'-succinates of AZT, 3TC and ABC and conjugated them to (PEG)CEPL nanogels to obtain polymer prodrugs. After sonication in aqueous solution, they formed compact cationic nanodrugs due to the formation of internal cholesterol clusters. In our studies, the plasma half-life of nanodrug was extended 3-fold and the clearance was reduced 2-fold compared to free AZT. (PEG)CEPL-sNRTI conjugates showed certain advantages compared to other types of polymeric conjugates such as mPEG-AZT prodrug, chitosan-d4T monophosphate conjugate or poly(HEMA-AZT) conjugate.<sup>26–28</sup> They demonstrated as particles more efficient accumulation in MDM and significant improvement of antiviral activity at the 90% HIV-1 suppression level (EC<sub>90</sub>) compared to free NRTIs. We attribute this superior antiviral efficacy to the assembly of new nanodrugs into compact particles in opposite to loose polymer coils of other drug conjugates. Assembled nanodrugs as pharmaceutical preparations also provide particle shape and size control, enhanced drug protection and better accumulation in macrophages.<sup>29</sup> Conversion of 3TC into an exocyclic amino group-protected prodrug increases drug stability against cytosine deamination *in vivo*. Inside macrophages, exocyclic amides can be effectively cleaved by cellular enzymes with restoration of active drug.<sup>30</sup>

Recently, several types of nanoassemblies were reported, e.g. squalenoylated (sc) dideoxycytidine (ddC) and didanosine (ddI), forming 100–300 nm micellar assemblies with

cholesteryl-PEG or sc-PEG, or poly-L-arginine-fatty acid derivatives of NRTIs that are capable of forming NPs with enhanced cell penetration.<sup>31, 32</sup> These nanoassemblies demonstrated a 2- to 3-fold decrease of the 50% effective doses (EC<sub>50</sub>) and anti-HIV activity at EC<sub>50</sub> was as low as 3  $\mu$ M. We obtained a similar or higher anti-HIV activity (EC<sub>90</sub>) using single nanodrugs and even better results for dual and triple nanodrug cocktails that imitate therapeutic Combivir and Trizivir cocktails.

Reported here new nanogel-NRTI conjugates presents a further step to more effective antiviral drugs for treatment of HIV-1 infection. Polymer-drug conjugates (prodrugs) proved to be efficient drug carriers with targeting abilities, as well as sustained drug release depots.<sup>33</sup> Drug release kinetics can be conveniently controlled by linker design. For example, we recently developed nanogel-nucleoside analog conjugates with polyphosphate linker that was stable even after oral administration.<sup>34</sup> NRTI prodrugs based on cationic  $\epsilon$ -polylysine are inexpensive and can be obtained using simple synthetic procedures. We also anticipate potential application of PEG-CEPL-sNRTI nanodrugs for more efficient therapy of HIV-1 infection in the CNS. Cationic nanogels with a PEG-CEPL backbone demonstrated in our previous studies an efficient transport across the blood-brain barrier (BBB) even without vectorization.<sup>14</sup> Vectorized nanodrugs will further advance the CNS delivery and allow to achieve a deeper suppression of HIV-1 infection in the brain. Lately, we demonstrated an effective targeting of antiviral nanodrugs to the brain using peptide vectors.<sup>9</sup> Multiple investigations of the fate of different NPs *in vivo* showed a strong dependence of brain accumulation efficacy on particle size.<sup>35</sup> Smaller metal NPs penetrate the BBB better and exhibit higher neurotoxicity. Smaller nanoparticles also migrate farther from capillaries into the brain parenchyma.<sup>36</sup> Hydrodynamic diameter range of the best CNS-penetrating nanoparticles was 20–70 nm. CEPL-sNRTI and PEGylated nanodrugs have been obtained in this size range and with narrow polydispersity. These properties are capable to increase drug delivery across the blood-brain barrier into brain-associated macrophages and microglial cells carrying HIV-1. Particle size also affects the retention of loaded cationic nanogels in bypassing organs; the maximum retention was observed for particles with the diameter between 100 and 200 nm. Smaller NPs will have a better chance to reach the brain endothelium, due to a lower retention in bypassing organs after *i.v.* administration. In conclusion, the new NRTI prodrugs in the form of nanogel-drug conjugates have several important advantages, which potentially allow them to enhance the efficacy of antiviral therapy, not only as the less toxic and less frequently administered alternative, but also as an effective targeted ART including CNS drug delivery and eradication of HIV-1 infection in the brain.

## Supplementary Material

Refer to Web version on PubMed Central for supplementary material.

## Acknowledgments

This research was supported with a R01 NS063879 grant to S.V.V from the National Institute of Neurodegenerative Diseases and Stroke (NINDS). The content is solely the responsibility of the authors and does not necessarily represent the official views of the National Institutes of Health (USA). The authors are grateful to Prof. Larisa Poluektova for help in planning and expert comments on the manuscript and, also, to Tom Bargar of Electron



Microscopy Core, Ed Ezell of NMR Core and Victoria Smith of Flow Cytometry Core Facilities at UNMC for valuable assistance.

## Abbreviations

<b>AZT</b>	Zidovudine
<b>3TC</b>	Lamivudine
<b>ABC</b>	Abacavir
<b>EPL</b>	$\epsilon$ -polylysine
<b>CEPL</b>	cholesteryl-EPL
<b>DCM</b>	dichloromethane
<b>TEA</b>	triethylamine
<b>CCF</b>	cholesteryl chloroformate
<b>EDC</b>	1-ethyl-3-(3-dimethylaminopropyl) carbodiimide
<b>HOBT</b>	hydroxybenzotriazole
<b>DMAP</b>	4-dimethylaminopyridine
<b>DCC</b>	N,N'-dicyclohexylcarbodiimide
<b>DMF</b>	dimethylformamide
<b>DMSO</b>	dimethyl sulfoxide
<b>DIPEA</b>	N,N'-diisopropylethylamine
<b>RhITC</b>	rhodamine B isothiocyanate
<b>MTT</b>	3-[4,5-dimethylthiazol-2-yl]-2,5-diphenyltetrazolium bromide
<b>NPs</b>	nanoparticles

## References

1. Margolis AM, Heverling H, Pham PA, Stolbach A. A review of the toxicity of HIV medications. *J Med Toxicol.* 2014; 10:26–39. [PubMed: 23963694]
2. Kabanov AV, Gendelman HE. Nanomedicine in the diagnosis and therapy of neurodegenerative disorders. *Prog Polym Sci.* 2007; 32:1054–1082. [PubMed: 20234846]
3. Sharma P, Garg S. Pure drug and polymer based nanotechnologies for the improved solubility, stability, bioavailability and targeting of anti-HIV drugs. *Adv Drug Deliv Rev.* 2010; 62:491–502. [PubMed: 19931328]
4. Lindl KA, Marks DR, Kolson DL, Jordan-Sciutto KL. HIV-associated neurocognitive disorder: pathogenesis and therapeutic opportunities. *J Neuroimmune Pharmacol.* 2010; 5:294–309. [PubMed: 20396973]
5. Kugelberg E. Capturing HIV infected T cells. *Nature Rev Immun.* 2015; 15:2–3.
6. Garden GA. Microglia in human immunodeficiency virus-associated neurodegeneration. *Glia.* 2002; 40:240–251. [PubMed: 12379911]
7. Abers MS, Shandera WX, Kass JS. Neurological and psychiatric adverse effects of antiretroviral drugs. *CNS Drugs.* 2014; 28:131–145. [PubMed: 24362768]

8. Warren G, Makarov E, Lu Y, Senanayake T, Rivera K, Gorantla S, Poluektova LY, Vinogradov SV. Amphiphilic cationic nanogels as brain-targeted carriers for activated nucleoside reverse transcriptase inhibitors. *J Neuroimmune Pharmacol.* 2015; 10:88–101. [PubMed: 25559020]
9. Gerson T, Makarov E, Senanayake TH, Gorantla S, Poluektova LY, Vinogradov SV. Nano-NRTIs demonstrate low neurotoxicity and high antiviral activity against HIV infection in the brain. *Nanomedicine.* 2014; 10:177–185. [PubMed: 23845925]
10. Vinogradov SV, Poluektova LY, Makarov E, Gerson T, Senanayake MT. Nano-NRTIs: efficient inhibitors of HIV type-1 in macrophages with a reduced mitochondrial toxicity. *Antivir Chem Chemother.* 2010; 21:1–14. [PubMed: 21045256]
11. Rehm BHA. Bacterial polymers: biosynthesis modifications and applications. *Nat Rev.* 2010; 8:578–598.
12. Nukuna A, Gendelman HE, Limoges J, Rasmussen J, Poluektova L, Ghorpade A, Persidsky Y. Levels of human immunodeficiency virus type 1 (HIV-1) replication in macrophages determines the severity of murine HIV-1 encephalitis. *J Neurovirol.* 2004; 10:82–90. [PubMed: 14982744]
13. Senanayake TH, Warren G, Wei X, Vinogradov SV. Application of activated nucleoside analogs for the treatment of drug-resistant tumors by oral delivery of nanogel-drug conjugates. *J Control Release.* 2013; 167:200–209. [PubMed: 23385032]
14. Vinogradov SV, Batrakova EV, Kabanov AV. Nanogels for oligonucleotide delivery to the brain. *Bioconjug Chem.* 2004; 15:50–60. [PubMed: 14733583]
15. Höschele D, Wiertz M, Garcia Moreno I. A duplex real-time PCR assay for detection of drug-induced mitochondrial DNA depletion in HepG2 cells. *Anal Biochem.* 2008; 379:208–10. [PubMed: 18541134]
16. Roy U, McMillan J, Alnouti Y, Gautum N, Smith N, Balkundi S, Dash P, Gorantla S, Martinez-Skinner A, Meza J, Kanmogne G, Swindells S, Cohen SM, Mosley RL, Poluektova L, Gendelman HE. Pharmacodynamic and antiretroviral activities of combination nanoformulated antiretrovirals in HIV-1-infected human peripheral blood lymphocyte-reconstituted mice. *J Infect Dis.* 2012; 206:1577–88. [PubMed: 22811299]
17. Ayers KM, Clive D, Tucker WE Jr, Hajian G, de Miranda P. Nonclinical toxicology studies with zidovudine: genetic toxicity tests and carcinogenicity bioassays in mice and rats. *Fundam Appl Toxicol.* 1996; 32:148–58. [PubMed: 8921318]
18. Giacalone G, Bochot A, Fattal E, Hillaireau H. Drug-induced nanocarrier assembly as a strategy for the cellular delivery of nucleotides and nucleotide analogues. *Biomacromol.* 2013; 14:737–742.
19. Sankar V, Nareshkumar PN, Ajitkumar GN, Penmetsa SD, Hariharan S. Comparative studies of lamivudine-zidovudine nanoparticles for the selective uptake by macrophages. *Curr Drug Deliv.* 2012; 9:506–514. [PubMed: 22452408]
20. Jorajuria S, Dereuddre-Bosquet N, Becher F, Martin S, Porcheray F, Garrigues A, Mabondzo A, Benech H, Grassi J, Orlowski S, Dormont D, Clayette P. ATP binding cassette multidrug transporters limit the anti-HIV activity of zidovudine and indinavir in infected human macrophages. *Antivir Ther.* 2004; 9:519–528. [PubMed: 15456083]
21. Zhang H, Gerson T, Varney ML, Singh RK, Vinogradov SV. Multifunctional peptide-PEG intercalating conjugates: programmatic of gene delivery to the blood-brain barrier. *Pharm Res.* 2010; 27:2528–2543. [PubMed: 20824308]
22. Giammona G, Cavallaro G, Pitarresi G. Studies of macromolecular prodrugs of zidovudine. *Adv Drug Deliv Rev.* 1999; 39:153–164. [PubMed: 10837772]
23. Vlieghe P, Clerc T, Pannecouque C, Witvrouw M, De Clercq E, Salles JP, Kraus JL. Synthesis of new covalently bound kappa-carrageenan-AZT conjugates with improved anti-HIV activities. *J Med Chem.* 2002; 45:1275–1283. [PubMed: 11881996]
24. Chimalakonda KC, Agarwal HK, Kumar A, Parang K, Mehvar R. Synthesis, analysis, in vitro characterization, and in vivo disposition of a lamivudine-dextran conjugate for selective antiviral delivery to the liver. *Bioconjug Chem.* 2007; 18:2097–2108. [PubMed: 17922546]
25. Wannachaiyasit S, Chanvorachote P, Nimmannit U. A novel anti-HIV dextrin-zidovudine conjugate improving the pharmacokinetics of zidovudine in rats. *AAPS Pharm Sci Tech.* 2008; 9:840–850.

26. Li W, Chang Y, Zhan P, Zhang N, Liu X, Pannecouque C, De Clercq E. Synthesis, in vitro and in vivo release kinetics, and anti-HIV activity of a sustained-release prodrug (mPEG-AZT) of 3'-azido-3'-deoxythymidine (AZT, Zidovudine). *Chem Med Chem*. 2010; 5:1893–1898. [PubMed: 20936623]
27. Yang L, Chen L, Zeng R, Li C, Qiao R, Hu L, Li Z. Synthesis, nanosizing and in vitro drug release of a novel anti-HIV polymeric prodrug: chitosan-O-isopropyl-5'-O-d4T monophosphate conjugate. *Bioorg Med Chem*. 2010; 18:117–123. [PubMed: 19959368]
28. Neeraj A, Chandrasekar MJ, Sara UV, Rohini A. Poly(HEMA-Zidovudine) conjugate: a macromolecular pro-drug for improvement in the biopharmaceutical properties of the drug. *Drug Deliv*. 2011; 18:272–280. [PubMed: 21110710]
29. Drummond DC, Zignani M, Leroux J. Current status of pH-sensitive liposomes in drug delivery. *Prog Lipid Res*. 2000; 39:409–460. [PubMed: 11082506]
30. Ferrero M, Gotor V. Biocatalytic selective modifications of conventional nucleosides carbocyclic nucleosides and C-nucleosides. *Chem Rev*. 2000; 100:4319–4348. [PubMed: 11749350]
31. Hillaireau H, Dereuddre-Bosquet N, Skanji R, Bekkara-Aounallah F, Caron J, Lepetre S, Argote S, Bauduin L, Yousfi R, Rogez-Kreuz C, Desmaele D, Rousseau B, Gref R, Andrieux K, Clayette P, Couvreur P. Anti-HIV efficacy and biodistribution of nucleoside reverse transcriptase inhibitors delivered as squalenoylated prodrug nanoassemblies. *Biomaterials*. 2013; 34:4831–4838. [PubMed: 23562054]
32. Pemmaraju BP, Malekar S, Agarwal HK, Tiwari RK, Oh D, Doncel GF, Worthen DR, Parang K. Design, synthesis, antiviral activity, and pre-formulation development of poly-L-arginine-fatty acyl derivatives of nucleoside reverse transcriptase inhibitors. *Nucleosides Nucleotides Nucleic Acids*. 2015; 34:1–15. [PubMed: 25513860]
33. Kopecek J. Polymer-drug conjugates: origins, progress to date and future directions. *Adv Drug Deliv Rev*. 2013; 65:49–59. [PubMed: 23123294]
34. Senanayake TH, Warren G, Vinogradov SV. Novel anticancer polymeric conjugates of activated nucleoside analogues. *Bioconjug Chem*. 2011; 22:1983–1993. [PubMed: 21863885]
35. Sonavane G, Tomoda K, Makino K. Biodistribution of colloidal gold nanoparticles after intravenous administration: effect of particle size. *Colloids Surf B Biointerfaces*. 2008; 66:274–280. [PubMed: 18722754]
36. Tzeng SY, Green JJ. Therapeutic nanomedicine for brain cancer. *Ther Deliv*. 2013; 4:687–704. [PubMed: 23738667]

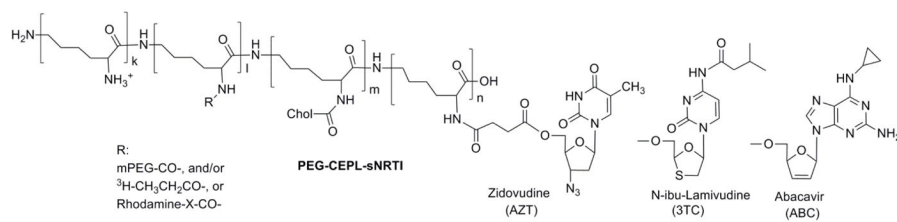


**Figure 1.**  
Chemical structure of antiviral (PEG) CEPL-sNRTI nanodrugs.

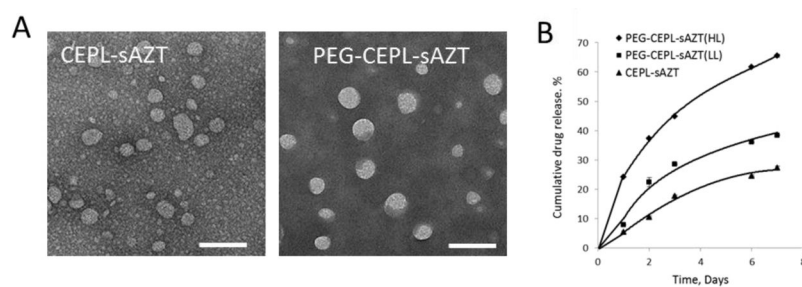


**Figure 2.**  
(A) TEM pictures of nanodrugs after vanadate staining. Bar: 100 nm. (B) *In vitro* drug release kinetics from different nanogel-AZT conjugates: CEPL-sAZT, PEG-CEPL-sAZT (LL) and PEG-CEPL-sAZT (HL) in PBS, 25°C.

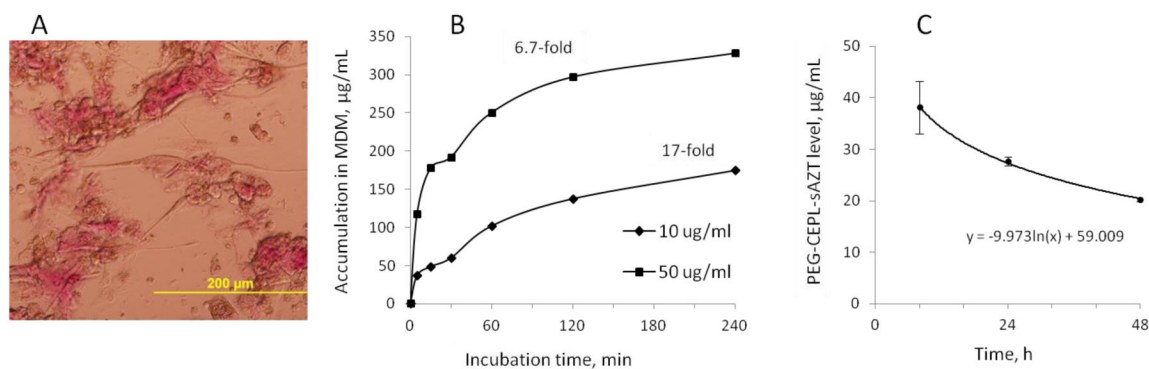


**Figure 3.**

(A) Fluorescent microimage of monocyte-derived macrophages (MDM) accumulating Rhodamine-tagged PEG-CEPL nanogel (50 µg/mL, 4 h at 37°C). (B) Kinetics of nanodrug accumulation in MDM ( $10^5$  cells) at different concentrations. The FACS data are converted to cellular concentration using a calibration curve for the fluorescent nanodrug. Cellular concentration of nanodrugs in MDM after 4 h-incubation increased 6.7- and 17-fold compared to the concentration in the treatment medium. (C) Kinetics of PEG-CEPL-sAZT content after uptake by MDM. Cells were incubated with nanodrug (0.5 mg/mL, 4 h at 37°C) and, then, the nanodrug level was determined at different time points by reverse phase HPLC.



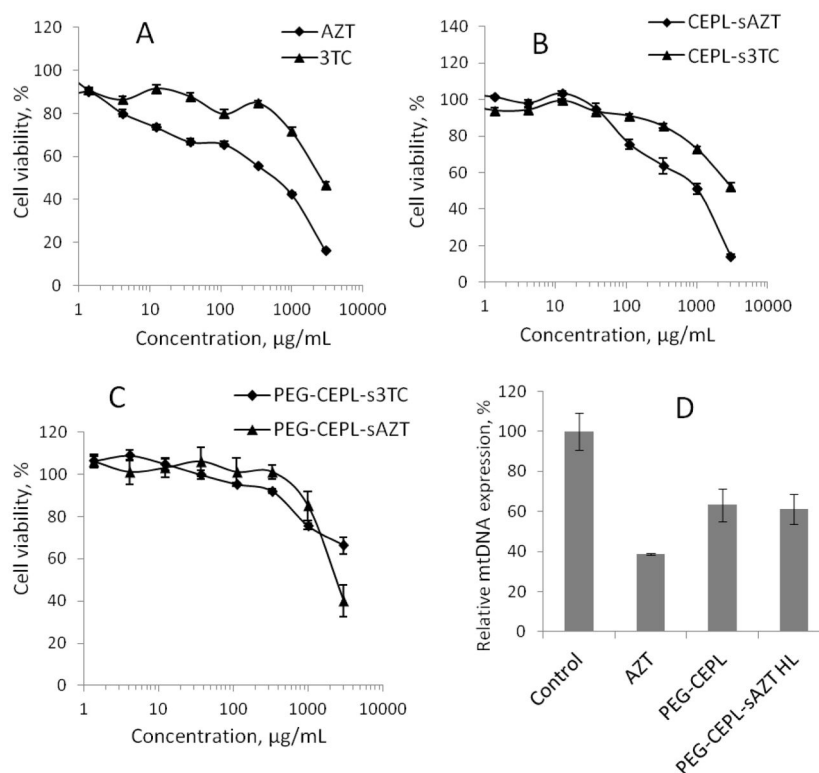


**Figure 4.**

Cytotoxicity of nanodrugs. Standard MTT assay was used to evaluate cytotoxicity of (A) NRTIs, (B) CEPL-sNRTI and (C) PEG-CEPL-sNRTI (HL) in macrophages (MDM). Cells were pretreated for 4 h with drugs or nanodrugs at different concentrations and incubated in fresh medium for 48 h. Cell viability was compared to non-treated cells (100%). Data show means  $\pm$  SEM (n = 8). (D) Mitochondrial toxicity of nanodrugs. Relative expression of mtDNA was calculated relatively to nuDNA using a real-time PCR after the treatment of HepG2 cells with AZT and AZT-equivalent doses of CEPL-sAZT and PEG-CEPL-sAZT. Cells were treated for 4 h on Days 1, 4 and 7 and, then, incubated in fresh medium at 37°C. Total DNA was isolated from non-treated control and treated cells on Day 10 and analyzed. Data show means  $\pm$  SEM (n = 4).

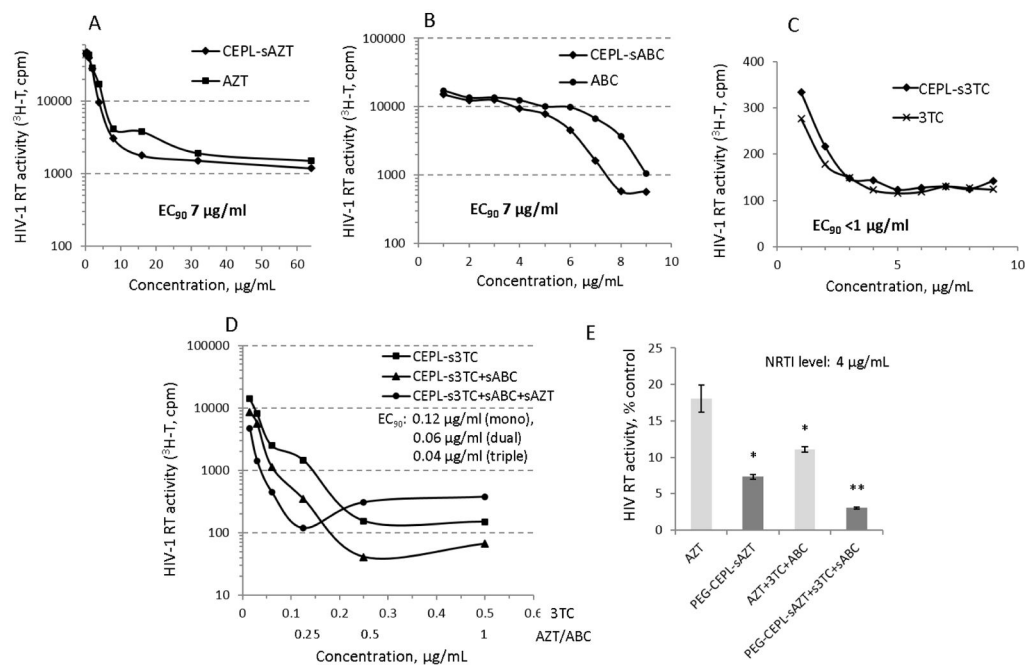


**Figure 5.**

Comparison of antiviral activity of NRTI, nanodrugs and nanodrug cocktails. HIV-1 reverse transcriptase (RT) activity was analyzed on Day 10 after infection by the inclusion of <sup>3</sup>H-thymidine. MDM cells were pretreated with nanodrugs or corresponding NRTI (A–C), or nanodrug cocktails (D) for 4 h before infection with HIV-1<sub>ADA</sub> virus (0.01 MOI). (E) PEG-CEPL-sAZT (LL) and the corresponding triple nanodrug cocktail were compared at the same total NRTI concentration 4 µg/mL in both groups. All data are shown as means (n = 5) normalized by viability (MTT assay) coefficients. Data variations between AZT-treated group and other groups in Figure 5E were statistically significant (\*, P < 0.05; \*\*, P < 0.01 by Student *t*-test).

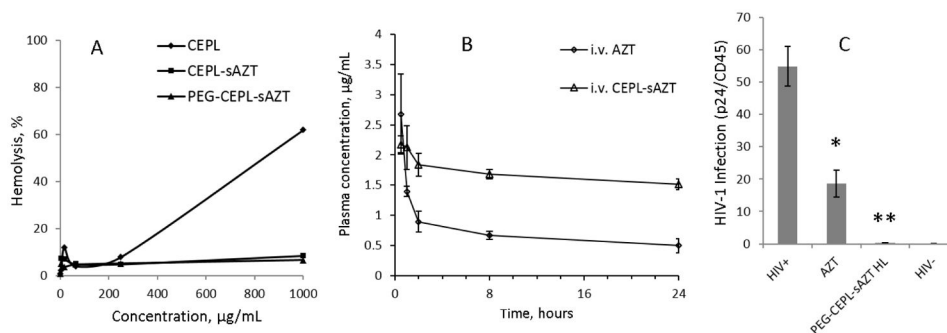


**Figure 6.** Hemolytic and pharmacokinetic properties, and antiviral efficacy of nanodrugs *in vivo*. (A) Hemolysis in the presence of nanodrugs. Red blood cells (RBC) were treated with nanodrugs for 30 min and the amount of released hemoglobin in supernatant after cell separation was measured by spectrometry. (B) Pharmacokinetic properties. Plasma concentration–time curve obtained after *i.v.* administration of 250 μg of <sup>3</sup>H-CEPL-sAZT. Data are shown as mean ± SD (n = 3). (C) Antiviral nanodrug activity in humanized hu-PBL mouse model of HIV-1 infection. Infected mice were treated with *i.v.* injections of PEG-CEPL-sAZT (HL) over 15 days (totally, three injections). Data are means ± SEM (n = 5). Data variations between non-treated infected (HIV+) group and treated infected groups were statistically significant (\*, P < 0.05; \*\*, P < 0.01 by Student *t*-test).

**Table 1**

Drug content and physicochemical properties of nanodrugs

Product	Drug content, %	Solubility, mg/mL	Particle size (d <sub>h</sub> ), nm <sup>*</sup>	Polydispersity (PDI) <sup>*</sup>	Zeta-potential, mV <sup>*</sup>
CEPL	-	-	15±7	0.27	55±5
PEG-CEPL	-	-	44±5	0.58	48±5
CEPL-sAZT	30	15	84±6	0.15	19±5
CEPL-sABC	21	12	96±5	0.14	30±6
CEPL-s3TC	28	20	19±9	0.53	14±5
PEG-CEPL-sAZT (LL)	14	>20	64±4	0.34	21±4
PEG-CEPL-sAZT (HL)	25	>20	45±9	0.57	18±4

\* Particle size (d<sub>h</sub>), polydispersity index (PDI) and zeta potential (ζ) were measured in 1% solutions in water after 2 h sonication. The results are average values ± SD of three measurements.

LL = lower drug loading, HL = higher drug loading.

**Table 2**

## Pharmacokinetic parameters

Parameters	CEPL-sAZT	AZT
Dose (mg/mouse)	0.25	0.075
T <sub>1/2</sub> (h)	115 ± 0.18	38 ± 0.06
AUC <sub>0-τ</sub> (h ng/mL)	132271 ± 863	22896 ± 85
AUC <sub>0-∞</sub> (h ng/mL)	212983 ± 1600	88404 ± 786
CL (mL/h)	1.92 ± 0.14	3.81 ± 0.17

\* Data are means ± SD. AZT content in CEPL-sAZT was 30% (wt). AZT release from the nanodrug was less than 5% during 24 h-incubation at 37°C.